Letter

Comparative study of magnetic quantum oscillations in Hall and transverse magnetoresistance

A. A. Sinchenko [1] P. D. Grigoriev [2,3,4] A. V. Frolov,[4] A. P. Orlov [4] V. N. Zverev [5]
A. Hadj-Azzem,[6] E. Pachoud,[6] and P. Monceau[6]

[1]*Laboratoire de Physique des Solides, Université Paris-Saclay*, CNRS, 91405 Orsay Cedex, France
[2]*L. D. Landau Institute for Theoretical Physics*, 142432 Chernogolovka, Russia
[3]*National University of Science and Technology "MISiS"*, 119049 Moscow, Russia
[4]*Kotelnikov Institute of Radioengineering and Electronics of RAS*, 125009 Moscow, Russia
[5]*Institute of Solid State Physics*, Chernogolovka, 142432 Moscow region, Russia
[6]*University Grenoble Alpes, Institute Neel*, F-38042 Grenoble, France
and CNRS, *Institute Neel*, F-38042 Grenoble, France

Magnetic quantum oscillations (MQO) provide a common tool to probe the electronic structure of various conductors. The Fermi surface of most metals is now known due to the MQO. This tool is more precise than its alternatives, but requires low temperatures, clean samples and rather strong magnetic fields. In this paper the MQO of Hall coefficient are measured in rare-earth tritelluride TmTe$_3$ and shown to be much stronger and persist to higher temperature than the Shubnikov-de Haas oscillations. This amplitude enhancement simplifies the MQO experiments and is very general in strongly anisotropic metals. The combined measurements of Hall and diagonal magnetoresistance provide additional useful information. The ratio of their MQO amplitudes depends linearly on magnetic field, and its slope gives a simple and accurate measurement tool of the electron mean free time and its temperature dependence, unachievable from the usual Dingle plot. Our results expand the use and applications of MQO as a powerful tool to investigate the electronic structure.

DOI: 10.1103/PhysRevB.110.L161108

The Landau quantization of electron spectrum in magnetic fields leads to the magnetic quantum oscillations (MQO) in metals [1–3]. Usually, the MQO are observed in magnetoresistance, called the Shubnikov-de Haas effect (ShdH), and in magnetization, called the de Haas-van Alphen effect (dHvA). These quantities are measured as a function of the inverse magnetic field and display a periodic behavior. The period is given by the extremal cross section of the Fermi surface (FS) encircled by conducting electrons in a semiclassical picture. The amplitude of the MQO is given by the well known Lifshitz-Kosevich (LK) formula [4]. This formula gives the relation between the MQO frequency and FS, and describes the MQO damping by thermal and disorder broadening. Fitting the experimental temperature dependence of MQO amplitude by the LK formula gives the effective electron mass m^*, while the field dependence of MQO amplitude gives the Landau-level (LL) broadening [1]. The MQO measurements provide a powerful tool to study the electronic properties of various quasi-two-dimensional (Q2D) layered metallic compounds which are the subject of intense studies now: organic metals [5,6], cuprate and iron-based high-temperature superconductors [7–14], heterostructures [15,16], graphite intercalation compounds [17], various van-der-Waal crystals [18], topological semimetals [19,23], etc.

Usually, only the diagonal component of magnetoresistance tensor is used to measure the MQO and to study the electronic structure, although the MQO of nondiagonal Hall component in some compounds may be much stronger and observable in a wider range of temperature, as it was reported for semiconductors [20]; semimetals HgTe and HgSe [21,22];

topological semimetals [23]; metal pentatellurides ZrTe$_5$ and HfTe$_5$ [24]; charge-density wave semimetal NbSe$_3$ [25]; and anomalous Hall resistance [26,27]. The MQO in the hole-doped high-Tc cuprate superconductors, giving new important knowledge about these compounds, were also first discovered measuring the Hall resistance [7]. When our paper was prepared, the MQO of Hall magnetoresistance component were also measured [28] in some rare-earth tritelluride compounds and found to be considerably larger than the MQO of diagonal component and more convenient for data analysis. However, one needs to know when this effect appears and how to use it properly. Therefore, it is interesting to compare the MQO of diagonal and Hall magnetoresistance components and to analyze what additional useful information it gives about the electronic structure. For this purpose we choose a Q2D compound TmTe$_3$ from the rare-earth tritellurides family which also demonstrates the effect of strong MQO in Hall resistance as it will be shown below.

Compounds of family RTe$_3$ (R = Y, La, Ce, Nd, Sm, Gd, Tb, Ho, Dy, Er, Tm) have weak orthorhombic structure (space group *Cmcm*) in the normal state [see Fig. 1(a)]. These systems exhibit a c-axis incommensurate charge-density wave (CDW) at high temperature through the whole R series that was recently a subject of intense studies [29–34]. For the heaviest rare-earth elements, a second a-axis CDW occurs at low temperature. MQO in RTe$_3$ compounds have been studied in works [28,35–39]. It was shown [39] that in RTe$_3$ compounds with the double CDW several small Fermi-surface pockets survive with a very small effective mass and with the largest area occupying only around 0.5% of the Brillouin
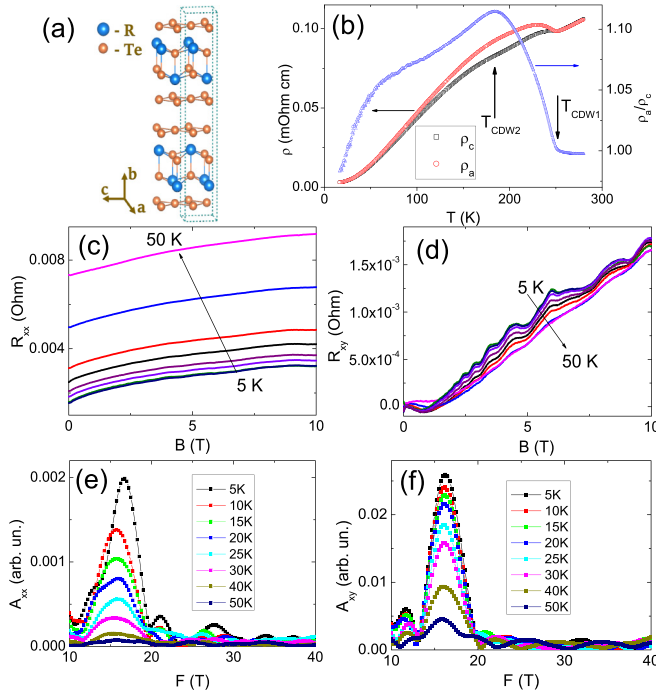
FIG. 1. (a) Crystal structure of RTe_3 compounds. (b) Temperature dependence of resistivity of $TmTe_3$ along the a and the c-axis directions and conductivity anisotropy, ρ_a/ρ_c, in the a-c plane. (c) Magnetoresistance, R_{xx}, and (d) Hall resistance, R_{xy}, in $TmTe_3$ as a function of magnetic field, B perpendicular to the (a-c) plane, at various temperatures in the range 5-50 K. (e) and (f) show the corresponding FFT.

zone. $TmTe_3$ is a member of the RTe_3 family with the heaviest rare-earth element and demonstrates the lowest transition temperature $T_{CDW1} = 250$ K of the first high-T CDW and the highest transition temperature $T_{CDW2} = 190$ K of the second low-T CDW [31]. Hence, $TmTe_3$ is most convenient for the comparative study of MQO in Hall and diagonal magnetoresistance because one may expect the appearance of MQO at not too strong magnetic field and at rather high temperature.

Single crystals of $TmTe_3$ were grown by a self-flux technique under purified argon atmosphere as described previously [32]. Thin single-crystal samples with a rectangular shape and with a thickness typically 1-2 μm were prepared by micromechanical exfoliation of relatively thick crystals glued on a sapphire substrate. RTe_3 compounds are quite sensitive to air, so the crystals should be stored in an oxygen- and moisture-free environment and all manipulation with the crystals in air should be done during minimal time. Because of this feature the electrical contacts were prepared by cold soldering of In. The magnetic field was applied parallel to the b axis, and in-plane magnetoresistance and the Hall resistance were recorded using the van der Pauw method [40], sweeping the field between $+10$ and -10 T. Measurements were performed at fixed temperature in the temperature range 4.2-100 K. Magnetic field dependencies of resistance and Hall resistance were determined as $\frac{(V(+B)\pm V(-B))}{2I}$ taking $(+)$ for magnetoresistance and $(-)$ for Hall resistance correspondingly. Conductivity measurements were performed using the Montgomery technique [41,42]. Electric transport

characteristics of the structures were measured using a Keithley 2400 precision current source and a Keysight 34420A nanovoltmeter. All measurements were carried out in an inert helium atmosphere.

Figure 1(b) shows the temperature dependence of resistivity of $TmTe_3$ measured along the in-plane c and a axes together with the anisotropy ratio ρ_a/ρ_c in the conducting ac plane using the Montgomery method. Above the Peierls transition temperature $T_{CDW1} = 270$ K the studied compound is practically isotropic in the ac plane and $\rho_a/\rho_c \approx 1$. Below T_{CDW1} the ratio ρ_a/ρ_c strongly increases in agreement with Ref. [33]. Below the second CDW transition temperature the resistivity anisotropy decreases, and at $T < 80$ K it becomes less than 5%. In this temperature range the compound can be considered as nearly isotropic in (ac) plane.

Figures 1(c) and 1(d) show the diagonal R_{xx} and Hall R_{xy} transverse magnetoresistance components in $TmTe_3$ as a function of magnetic field B at various temperatures T in the range 5-50 K. The MQO of R_{xy} are much more pronounced than of those of R_{xx}. Panels (e) and (f) demonstrate the corresponding Fourier transforms (FFT) in the window 3-9 T for MQO of resistivity components ρ_{xx} and ρ_{xy}. The MQO with frequency $F = 15$ T clearly manifest in both the diagonal and Hall magnetoresistance. However, the MQO of Hall resistivity are much stronger and observable till considerably higher temperature in accordance with results of work [28].

The temperature dependence of MQO amplitude $A(T, B)$ is used to extract the effective electron mass m^*, and its field dependence gives the Dingle temperature $T_D = \hbar/2\pi k_B\tau$, related to the electron mean free time τ, where $k_B = 1.38 \cdot 10^{-16}$ erg/K is the Boltzmann's constant. In 2D metals the amplitude of MQO is described by modified Lifshitz-Kosevitch formula [43]:

$$A(T, B) \propto R_T(T, B)R_D(B), \quad (1)$$

where the temperature damping factor

$$R_T = R_T(T, B) = \frac{\lambda}{\sinh(\lambda)}, \quad \lambda \equiv \frac{2\pi k_B T}{\hbar\omega_c}, \quad (2)$$

$\omega_c = eB/m^*c$ is the cyclotron frequency, e is the electron charge, and c is the light velocity. The damping of MQO by disorder is described by the usual Dingle factor

$$R_D = \exp\left(-\frac{2\pi^2 k_B T_D}{\hbar\omega_c}\right) = \exp\left(-\frac{\pi}{\omega_c\tau}\right). \quad (3)$$

The magnetic oscillations of diagonal and Hall magnetoresistance at different temperatures are shown in Figs. 2(a) and 2(b) correspondingly. To determine the amplitudes of oscillation at $F = 15$ T more accurately, especially at high temperature, we used the bandpass filtering in square window between $F_1 = 10$ T and $F_2 = 20$ T for all the temperatures. Then, applying the inverse Fourier transformation [44,45] we succeeded to trace the amplitude of oscillation in a wider range of magnetic field. Figure 2(c) demonstrates the temperature evolution of MQO amplitudes. The MQO amplitude A_{xx} of the diagonal magnetoresistance (blue symbols) is well fitted by the Eq. (1) (blue solid lines) with the best-fit value $m^*_\alpha = 0.033m_e$. The low ShdH frequency and very small effective mass indicate the existence of small FS pockets with very light carriers in these compounds at low T in agreement with
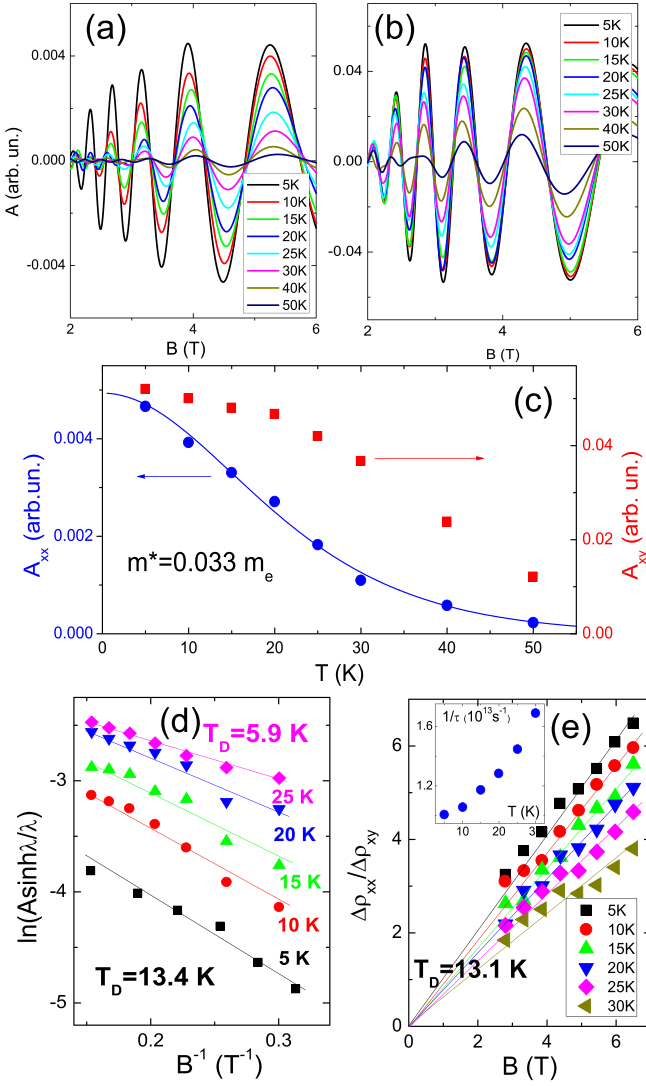
FIG. 2. Temperature evolution of the MQO of magnetoresistance (a) and of Hall resistance (b) in TmTe$_3$ for $F = 15$ T. (c) The temperature dependence of the amplitude of Shubnikov oscillations for $F = 15$ T (blue symbols) and the corresponding Lifshitz-Kosevitch fits (blue solid lines). Red squares indicate the temperature dependence of MQO amplitude of the Hall resistance. (d) The Dingle plots, $\ln(A \sinh(\lambda)/\lambda)(B^{-1})$, for the MQO of diagonal magnetoresistance ρ_{xx} at the same temperatures. (e) The magnetic-field dependence of the ratio of MQO amplitudes, A_{xx}/A_{xy}, at various temperatures. Inset shows the corresponding temperature dependence of the scattering rate, $1/\tau(T)$.

Ref. [39]. At the same time, the temperature dependence of the oscillation amplitude A_{xy} of Hall resistance, indicated by red squares in Fig. 2(c), cannot be described by the same formula because A_{xy} decreases much slower than A_{xx} as temperature grows and the MQO of ρ_{xy} are observable up to much higher temperatures.

The Dingle temperature and the scattering time are, usually, extracted from the so-called Dingle plot that is the logarithm of MQO amplitude divided by a thermal damping factor (2), $R_T = \lambda/\sinh(\lambda)$, plotted as a function of inverse magnetic field, $1/B$. The corresponding Dingle plots for the

MQO of ρ_{xx} are shown in Fig. 2(d) at various temperatures. We see that these plots and their slope change strongly as temperature increases. The Dingle temperature extracted from the slope of these curves at $T = 5$ K is equal to $T_D \approx 13.4$ K, while at $T = 25$ K it decreases to $T_D \approx 5.9$ K. Of course, this strong decrease of $T_D(T)$ is not physical and appears from the incorrect use of Eqs. (1) and (2) beyond their applicability region. As we argue below, one may use the value T_D extracted only at low temperature. The corresponding scattering times extracted from the Dingle plot at low $T = 5$ K is $\tau_\alpha = (0.90 \pm 0.07) \cdot 10^{-13}$ seconds.

The MQO of magnetoresistance in two-dimensional (2D) electron systems for low/intermediate magnetic fields were theoretically studied in Ref. [46]. According to this work, the MQO should be observable both in diagonal and Hall magnetoresistance components, and for one-band 2D metals they are given by simple formulas:

$$\rho_{xx} = \frac{1}{\sigma_0}\left(1 + 2\frac{\Delta g(T)}{g_0}\right), \qquad (4)$$

$$\rho_{xy} = \frac{\omega_c \tau}{\sigma_0}\left(1 - \frac{1}{(\omega_c \tau)^2}\frac{\Delta g(T)}{g_0}\right), \qquad (5)$$

where in a weak magnetic field, when high harmonics of MQO are small,

$$\frac{\Delta g(T)}{g_0} = -2\cos\left(\frac{2\pi \varepsilon_F}{\hbar \omega_c}\right)R_D R_T \qquad (6)$$

is the oscillatory part of the density of states (DoS), multiplied by the temperature damping factor R_T, ε_F is the Fermi energy, and the damping factors R_D and R_T are given by Eqs. (3) and (2). Equations (4)–(6) were recently generalized [47,48] to layered quasi-2D metals (see Eqs. (57)–(60) of Ref. [47]) and shown to be valid in the main (first) order in the Dingle factor R_D even at finite interlayer electron transfer integral t_z if the oscillating DoS in Eq. (6) is multiplied by the additional factor $J_0(4\pi t_z/(\hbar \omega_c))$ typical to quasi-2D metals, where $J_0(x)$ is the Bessel function of zeroth order. According to Ref. [31] the conductivity anisotropy along and across the conducting layers in TmTe$_3$ and other rare-earth tritellurides at low T is larger than 10^2. Hence, the use of quasi-2D model is justified in our case.

Equations (4) and (5) are derived using the Feynman diagram technique in a quantizing magnetic field, namely, the Kubo and Kubo-Streda formulas (see Refs. [46,47] for more details). They are quite simple because they are obtained in the first order of MQO amplitude and for single-band metals. The first limitation is, usually, justified when the first MQO harmonic is much stronger than higher harmonics, but the second condition is often not fulfilled. Unfortunately, the similar calculation for multiband metals is rather cumbersome. We performed the similar calculation using the Kubo and Kubo-Streda formulas for two-band metals with close cyclotron frequencies ω_c [49]. When two Fermi-surface pockets are of the same type (both electron or both hole-type), the single-band result is confirmed by these calculations. When the carrier types differ (electrons and holes), the structure of Eqs. (4) and (5) does not change, but the coefficients before the oscillating and nonoscillating terms in the round brackets do change. The latter is not surprising because the

nonoscillating part of Hall coefficient contains a difference of the contributions from electrons and holes. The detailed formula depends on the electron density and dispersion in the electron and hole pockets, as well as on the difference between intra- and intersubband electron scattering. Typically, the MQO amplitude A_{xy} of Hall resistivity get even more enhanced as compared to A_{xx} than in Eqs. (4) and (5). Therefore, the main conclusions from Eqs. (4) and (5) about the larger amplitude and weaker temperature dependence of magnetic quantum oscillations of Hall magnetoresistance components as compared to the diagonal one remains valid in multiband metals.

Now the fact that the observed MQO in Hall resistance ρ_{xy} are stronger and observable up to much higher temperatures than the MQO of ρ_{xx} is not surprising because it directly follows from Eqs. (4) and (5). Indeed, in contrast to MQO of ρ_{xx} the amplitude A_{xy} of MQO in ρ_{xy} is inversely proportional to τ_0, which should decrease as the temperature grows because the electron levels become broadened not only by static crystal disorder but also by thermal excitations due to the electron-phonon (e-ph) and electron-electron (e-e) interaction.

We now emphasize another interesting point: Equations (4) and (5) predict a very simple formula for the ratio of MQO amplitudes,

$$\Delta\rho_{xx}/\Delta\rho_{xy} = 2\omega_c\tau = 2eB\tau/(m^*c). \qquad (7)$$

Hence, plotting the ratio $\Delta\rho_{xx}/\Delta\rho_{xy}$ as a function of magnetic field B one obtains a linear dependence with a slope equal to $2e\tau/(m^*c)$. Figures 2(a) and 2(b) show the magnetic-field dependence of the relative MQO amplitudes $\Delta\rho_{xx}/\bar{\rho}_{xx}$ and $\Delta\rho_{xy}/\bar{\rho}_{xy}$ obtained from the inverse Fourier transformation, where $\bar{\rho}_{xx}$ and $\bar{\rho}_{xy}$ are nonoscillating parts of diagonal and Hall magnetoresistivity correspondingly.

The Hall-resistivity oscillations are almost in antiphase to magnetoresistance oscillations [see Figs. 2(a) and 2(b)], which corresponds to the theoretical prediction [46,47] in Eqs. (4) and (5). In Fig. 2(e) the ratio of the absolute values of MQO amplitudes, $\Delta\rho_{xx}/\Delta\rho_{xy}$, as a function of B are shown at various temperatures. We see that these dependencies are linear at all temperatures in agreement with Eq. (7). The scattering time obtained using Eq. (7) from the slope of this curve at $T = 5$ K is $\tau = (0.99 \pm 0.09) \cdot 10^{-13}$ s, which coincides with the scattering time $\tau_\alpha = (0.90 \pm 0.07) \cdot 10^{-13}$ s extracted from the Dingle plot at the same temperature.

The above results suggest a new and elegant method to determine the electron scattering time τ using the ratio between the MQO amplitudes of diagonal and Hall magnetoresistivity. To check the applicability region of the proposed method we apply it at higher temperatures and compare with other common methods. As we noted before, the Dingle plots at $T > 10$ K demonstrate an unrealistic behavior. For $T = 5, 10, 15, 20, 25$ K these plots are shown in Fig. 2(d), where all these graphs are almost linear but with a slope that continuously decreases with increasing temperature. This corresponds to the decrease of scattering time $\tau(T)$ with increasing temperature, which is unphysical and indicates that the L-K formula (1),(2) for the temperature dependence of MQO amplitude does not hold. At $T = 5$ K the temperature damping factor R_T is only a small correction that does

not affect the Dingle plot. Hence, the extracted Dingle temperature $T_D = 13.4$ K and the corresponding mean-free time $\tau_\alpha \approx 0.9 \cdot 10^{-13}$ s are reasonable. However, at higher temperature even small violations of the L-K formula (1) change dramatically the final Dingle plot and spoil the common method of determining τ from the Dingle plot. The precise temperature dependence of MQO amplitude, required for a correct Dingle plot at finite T, needs a more detailed theoretical study and calculations, which are beyond the scope our paper.

In contrast, we can extract the scattering time τ at high temperature from the ratio $\Delta\rho_{xx}/\Delta\rho_{xy}$. The dependence of this ratio on magnetic field B at $T = 5, 10, 15, 20, 25, 30$ K is shown in Fig. 2(e). In contrast to the Dingle-plot procedure, from the ratios $\Delta\rho_{xx}/\Delta\rho_{xy}$ we obtain a reasonable temperature dependence of the scattering rate $1/\tau(T)$ shown in the inset in Fig. 2(e) and given by the sum of contributions from the electron-phonon (e-ph) and electron-electron (e-e) interaction [2],

$$\tau^{-1}(T) = \tau^{-1}(0) + \tau_{\text{e-ph}}^{-1}(T) + \tau_{e-e}^{-1}(T), \qquad (8)$$

where at low $T < 30$K $\tau_{\text{e-ph}}^{-1}(T) \propto T^3$ and $\tau_{e-e}^{-1}(T) \propto T^2$. Note that the temperature dependence of scattering time, obtained fitting the experimental data using Eq. (7) and shown in the inset in Fig. 2(e), reasonably agrees with the temperature dependence of resistivity and qualitatively with Eq. (8). This suggests that the short-range scattering potential, coming from impurities or other crystal imperfections or from short-wavelength phonons, gives the major contribution to the electron scattering rate in this temperature range, but the e-e and e-ph interaction is also considerable at $T > 10$K.

With increasing temperature, the MQO in magnetoresistance quickly disappear according to Eq. (2) due to temperature smearing of the Fermi level. An increase in temperature also leads to the raise of electron scattering rate τ^{-1} because of the e-ph and e-e interaction [2]. However, in the lowest order of e-ph interaction and for exponentially weak MQO, the e-ph interaction leaves the Dingle factor R_D and the effective mass m^* unchanged in the MQO damping given by Eq. (1) [50,51]. This comes from the special cancellation of two terms in the electron self energy at $T \gg \hbar\omega_c$, which enter both R_D and R_T. Later this cancellation was confirmed for the 2D electron systems and for the e-e interaction [52–54] and named the first Matsubara-frequency rule [54].

The above cancellation of the T-dependence of MQO amplitude [50–54] concerns only the exponential factor given by Eq. (1), which contains the product of R_T and R_D. The prefactors $\omega_c\tau$ in Eqs. (5) and (7), as well as the Dingle factor R_D alone, do not have this cancellation, and τ in these prefactors depends on temperature.

The resistivity $\rho_{xx}(T)$ contains the T-dependence of the transport scattering rate $\tau_{tr}^{-1}(T)$, which differs from $\tau^{-1}(T)$ at low temperature [2]. Hence, $\rho_{xx}(T)$ only gives a qualitative dependence $\tau(T)$. Thermal conductivity contains $\tau^{-1}(T)$ in combination with the electronic part of the specific heat $C(T) \propto T$ [2] and also can be used to extract the dependence $\tau^{-1}(T)$. The temperature dependence of τ and of the Dingle factor (3) can also be studied experimentally using the so-called differential or slow magnetoresistance oscillations

(SlO) [36,48,55–58]

$$\rho_d \approx A_d \cos\left(2\pi\,\Delta F/B\right)R_D^2 \tag{9}$$

with a frequency ΔF proportional not to the Fermi energy ε_F or to the Fermi-pocket area but to the splitting of electron band structure due to the interlayer transfer integral. This energy splitting is not affected by the temperature smearing of the Fermi level, hence the SlO do not have the temperature damping factor R_T given by Eq. (2), and the temperature damping of SlO is determined only by the electron scattering processes entering $\tau^{-1}(T)$. The SlO amplitude is also not affected by the macroscopic sample inhomogeneities, which smear the Fermi level and MQO similar to temperature [48,55–59]. Therefore, the SlO are often stronger than the usual MQO [55]. The magnetic intersubband oscillations [60–63] or difference-frequency oscillations in multiband metals [64] have a similar origin but are less convenient to extract $\tau^{-1}(T)$, since their amplitudes contain the temperature damping factor $R_T(T)$ because the effective masses differ on two different bands or FS pockets.

We pay attention on the fact which was not seen before: if τ in Eq. (5) decreases with temperature, e.g., due to e-e or e-ph interaction, the MQO should fade with temperature much slower for Hall than for diagonal resistivity, because the oscillatory term in Hall resistivity is inversely proportional τ. This interesting fact did not get enough attention till now, probably, because the work [46] was oriented mainly on the quantum Hall effect (QHE) systems. As a rule, QHE is studied in semiconducting heterostructures having relatively low carrier concentration. Hence, in these structures the relative MQO in Hall resistance appear much weaker than the MQO in magnetoresistance. Another situation takes place in metallic Q2D compounds where the carrier concentration is high and the Hall effect is not too large. In such systems one can expect that the relative MQO in Hall coefficient are much stronger than in diagonal magnetoresistance. As an indication of such a behavior we notice the first observation of MQO in high-temperature cuprate superconductors just in the Hall resistance [7]. From Eq. (5) we see that the MQO of Hall coefficient are stronger than the MQO of diagonal magnetoresistance at low and intermediate magnetic field range when $\omega_c\tau \lesssim 1$. Thus, for the experimental observation of this enhancement of MQO in Hall coefficient in other compounds, the most convenient is to study Q2D metals in the intermediate magnetic-field range.

To summarize, we performed a comprehensive analysis of the quantum oscillations of magnetoresistance tensor in layered rare-earth tritellurides, including the intralayer diagonal and Hall magnetoresistance. The magnetic quantum oscillations (MQO) of Hall coefficient are much stronger and persist to much higher temperature. We show that this is a general effect for MQO in highly anisotropic metals, and the combined Hall and diagonal magnetoresistance measurements provide additional useful information about the electronic structure. In particular, the ratio of MQO amplitudes of diagonal and Hall magnetoresistance components depends linearly on the magnetic field, and its slope gives a simpler and much more accurate estimate of the electron mean free time than the Dingle plot, especially at finite temperature $T \sim \hbar\omega_c$. This provides an elegant new method of measuring the electron scattering rate and its temperature dependence in various quasi-2D conductors, including high-temperature superconductors, organic metals, layered van-der-Waal crystals, topological materials, graphite intercalation compounds, artificial heterostructures, etc.

[1] D. Shoenberg, *Magnetic Oscillations in Metals* (Cambridge University Press, Cambridge, 1984).

[2] A. A. Abrikosov, *Fundamentals of the Theory of Metals* (North-Holland, Amsterdam, 1988).

[3] J. M. Ziman, *Principles of the Theory of Solids* (Cambridge University Press, Cambridge, 1972).

[4] I. M. Lifshitz and A. M. Kosevich, Theory of magnetic susceptibility in metals at low temperatures, Sov. Phys. JETP **2**, 636 (1955).

[5] *The Physics of Organic Superconductors and Conductors*, edited by A. G. Lebed, Springer Series in Materials Science Vol. 110 (Springer-Verlag, Berlin, Heidelberg, 2008).

[6] M. V. Kartsovnik, High magnetic fields: A tool for studying electronic properties of layered organic metals, Chem. Rev. **104**, 5737 (2004).

[7] N. Doiron-Leyraud, C. Proust, D. LeBoeuf, J. Levallois, J.-B. Bonnemaison, R. Liang, D. A. Bonn, W. N. Hardy, and L. Taillefer, Quantum oscillations and the Fermi surface in an underdoped high-T_c superconductor, Nature (London) **447**, 565 (2007).

[8] B. Vignolle, A. Carrington, R. A. Cooper, M. M. J. French, A. P. Mackenzie, C. Jaudet, D. Vignolles, C. Proust, and N. E. Hussey, Quantum oscillations in an overdoped high-T_c superconductor, Nature (London) **455**, 952 (2008).

[9] T. Helm, M. V. Kartsovnik, M. Bartkowiak, N. Bittner, M. Lambacher, A. Erb, J. Wosnitza, and R. Gross, Evolution of the Fermi surface of the electron-doped high-temperature superconductor $Nd_{2-x}Ce_xCuO_4$ revealed by Shubnikov–de Haas oscillations, Phys. Rev. Lett. **103**, 157002 (2009).

[10] T. Helm, M. V. Kartsovnik, I. Sheikin, M. Bartkowiak, F. Wolff-Fabris, N. Bittner, W. Biberacher, M. Lambacher, A. Erb, J. Wosnitza, and R. Gross, Magnetic breakdown in the electron-doped cuprate superconductor $Nd_{2-x}Ce_xCuO_4$: The reconstructed Fermi surface survives in the strongly overdoped regime, Phys. Rev. Lett. **105**, 247002 (2010).

[11] S. E. Sebastian, N. Harrison, R. Liang, D. A. Bonn, W. N. Hardy, C. H. Mielke, and G. G. Lonzarich, Quantum oscillations from nodal bilayer magnetic breakdown in the underdoped high temperature superconductor $YBa_2Cu_3O_{6+x}$, Phys. Rev. Lett. **108**, 196403 (2012).

[12] T. Terashima, N. Kurita, M. Tomita, K. Kihou, C.-H. Lee, Y. Tomioka, T. Ito, A. Iyo, H. Eisaki, T. Liang, M. Nakajima, S. Ishida, Shin-ichi Uchida, H. Harima, and S. Uji, Complete Fermi surface in $BaFe_2As_2$ observed via Shubnikov–de

Haas oscillation measurements on detwinned single crystals, Phys. Rev. Lett. **107**, 176402 (2011).

[13] D. Graf, R. Stillwell, T. P. Murphy, J.-H. Park, E. C. Palm, P. Schlottmann, R. D. McDonald, J. G. Analytis, I. R. Fisher, and S. W. Tozer, Pressure dependence of the $BaFe_2As_2$ Fermi surface within the spin density wave state, Phys. Rev. B **85**, 134503 (2012).

[14] A. I. Coldea, D. Braithwaite, and A. Carrington, Iron-based superconductors in high magnetic fields, Comptes Rendus. Physique **14**, 94 (2013).

[15] M. Kuraguchi, E. Ohmichi, T. Osada, and Y. Shiraki, Interlayer coherency and angular-dependent magnetoresistance oscillations in quasi-two-dimensional conductors, Synth. Met. **133-134**, 113 (2003).

[16] Y.-W. Tan, H. L. Stormer, L. N. Pfeiffer, and K. W. West, High-frequency magneto-oscillations in GaAs/AlGaAs quantum wells, Phys. Rev. Lett. **98**, 036804 (2007).

[17] G. Csanyi, P. B. Littlewood, A. H. Nevidomskyy, C. J. Pickard, and B. D. Simon, The role of the interlayer state in the electronic structure of superconducting graphite intercalated compounds, Nat. Phys. **1**, 42 (2005).

[18] B. Fallahazad, H. C. P. Movva, K. Kim, S. Larentis, T. Taniguchi, K. Watanabe, S. K. Banerjee, and E. Tutuc, Shubnikov-de Haas oscillations of high-mobility holes in monolayer and bilayer WSe_2: Landau level degeneracy, effective mass, and negative compressibility, Phys. Rev. Lett. **116**, 086601 (2016).

[19] Q. Jiang, C. Wang, P. Malinowski, Z. Liu, Y. Shi, Z. Lin, Z. Fei, T. Song, D. Graf, S. Chikara, X. Xu, J. Yan, D. Xiao, and J.-H. Chu, Quantum oscillations in the field-induced ferromagnetic state of $MnBi_{2-x}Sb_xTe_4$, Phys. Rev. B **103**, 205111 (2021).

[20] G. M. Minkov, O. E. Rut, A. A. Sherstobitov, S. A. Dvoretski, N. N. Mikhailov, and A. V. Germanenko, Quantum oscillations of transport coefficients and capacitance: A manifestation of the spin Hall effect, Phys. Rev. B **108**, 075301 (2023).

[21] R. A. Stradling and G. A. Antcliffe, Magnetoresistance Studies of HgTe at low temperatures, J. Phys. Soc. Japan **21**, 374 (1966) Supplement.

[22] L. M. Bliek and G. Landwehr, De Haas-Van Alphen and Shubnikov-De Haas effect in n-HgSe in strong magnetic fields, Phys. Status Solidi (b) **31**, 115 (1969).

[23] M. Busch, O. Chiatti, S. Pezzini, S. Wiedmann, J. Sánchez-Barriga, O. Rader, L. V. Yashina, and S. F. Fischer, High-temperature quantum oscillations of the Hall resistance in bulk Bi_2Se_3, Sci. Rep. **8**, 485 (2018).

[24] Q. Xie, C. Wang, S. Yan, L. Chen, J. Zheng, and W. Wang, Quantum oscillations and stacked quantum Hall effect in $HfTe_5$, Appl. Phys. Lett. **120**, 141903 (2022).

[25] R. V. Coleman, M. P. Everson, H.-A. Lu, A. Johnson, and L. M. Falicov, Effects of high magnetic fields on charge-density waves in $NbSe_3$, Phys. Rev. B **41**, 460 (1990).

[26] A. T. Lonchakov, S. B. Bobin, V. V. Deryushkin, V. I. Okulov, T. E. Govorkova, V. N. Neverov, E. A. Pamyatnykh, and L. D. Paranchich, Experimental detection of quantum oscillations of anomalous Hall resistance in mercury selenide crystals with cobalt impurities, Low Temp. Phys. **43**, 504 (2017).

[27] V. Yu. Tsaran and S. G. Sharapov, Magnetic oscillations of the anomalous Hall conductivity, Phys. Rev. B **93**, 075430 (2016).

[28] T. Higashihara, R. Asama, R. Nakamura, M. Watanabe, N. Tomoda, T. J. Hasiweder, Y. Fujisawa, Y. Okada, T. Iwasaki, K. Watanabe, T. Taniguchi, N. Jiang, and Y. Niimi, Magneto-transport properties in van der Waals RTe_3 (R=La, Ce, Tb), Phys. Rev. B **109**, 134404 (2024).

[29] E. DiMasi, M. C. Aronson, J. F. Mansfield, B. Foran, and S. Lee, Chemical pressure and charge-density waves in rare-earth tritellurides, Phys. Rev. B **52**, 14516 (1995).

[30] V. Brouet, W. L. Yang, X. J. Zhou, Z. Hussain, R. G. Moore, R. He, D. H. Lu, Z. X. Shen, J. Laverock, S. B. Dugdale, N. Ru, and I. R. Fisher, Angle-resolved photoemission study of the evolution of band structure and charge density wave properties in RTe_3 (R=Y, La, Ce, Sm, Gd, Tb, and Dy), Phys. Rev. B **77**, 235104 (2008).

[31] N. Ru, C. L. Condron, G. Y. Margulis, K. Y. Shin, J. Laverock, S. B. Dugdale, M. F. Toney, and I. R. Fisher, Effect of chemical pressure on the charge density wave transition in rare-earth tritellurides RTe_3, Phys. Rev. B **77**, 035114 (2008).

[32] A. A. Sinchenko, P. Lejay, and P. Monceau, Sliding charge-density wave in two-dimensional rare-earth tellurides, Phys. Rev. B **85**, 241104(R) (2012).

[33] A. A. Sinchenko, P. D. Grigoriev, P. Lejay, and P. Monceau, Spontaneous breaking of isotropy observed in the electronic transport of rare-earth tritellurides, Phys. Rev. Lett. **112**, 036601 (2014).

[34] A. A. Sinchenko, P. Lejay, O. Leynaud, and P. Monceau, Unidirectional charge-density-wave sliding in two-dimensional rare-earth tritellurides, Solid State Commun. **188**, 67 (2014).

[35] N. Ru, R. A. Borzi, A. Rost, A. P. Mackenzie, J. Laverock, S. B. Dugdale, and I. R. Fisher, De Haas–van Alphen oscillations in the charge density wave compound lanthanum tritelluride $LaTe_3$, Phys. Rev. B **78**, 045123 (2008).

[36] P. D. Grigoriev, A. A. Sinchenko, P. Lejay, A. Hadj-Azzem, J. Balay, O. Leynaud, V. N. Zverev, and P. Monceau, Bilayer splitting versus Fermi-surface warping as an origin of slow oscillations of in-plane magnetoresistance in rare-earth tritellurides, Eur. Phys. J. B **89**, 151 (2016).

[37] S. Lei, J. Lin, Y. Jia, M. Gray, A. Topp, G. Farahi, S. Klemenz, T. Gao, F. Rodolakis, J. L. McChesney, C. R. Ast, A. Yazdani, K. S. Burch, S. Wu, N. P. Ong, and L. M. Schoop, High mobility in a van der Waals layered antiferromagnetic metal, Sci. Adv. **6**, eaay6407 (2020).

[38] M. Watanabe, S. Lee, T. Asano, T. Ibe, M. Tokuda, H. Taniguchi, D. Ueta, Y. Okada, K. Kobayashi, and Y. Niimi, Quantum oscillations with magnetic hysteresis observed in $CeTe_3$ thin films, Appl. Phys. Lett. **117**, 072403 (2020).

[39] P. Walmsley, S. Aeschlimann, J. A. W. Straquadine, P. Giraldo-Gallo, S. C. Riggs, M. K. Chan, R. D. McDonald, and I. R. Fisher, Magnetic breakdown and charge density wave formation: A quantum oscillation study of the rare-earth tritellurides, Phys. Rev. B **102**, 045150 (2020).

[40] L. J. van der Pauw, Determination of the resistivity tensor and Hall tensor of anisotropic conductors, Philips Res. Repts. **16**, 187 (1961).

[41] H. C. Montgomery, Method for measuring electrical resistivity of anisotropic materials, J. Appl.Phys. **42**, 2971 (1971).

[42] B. F. Logan, S. O. Rice, and R. F. Wick, Series for computing current flow in a rectangular block, J. Appl. Phys. **42**, 2975 (1971).

[43] D. Shoenberg, Magnetization of a two-dimensional electron gas, J. Low Temp. Phys. **56**, 417 (1984).

[44] B. Habib, E. Tutuc, S. Melinte, M. Shayegan, D. Wasserman, S. A. Lyon, and R. Winkler, Spin splitting in GaAs (100) two-dimensional holes, Phys. Rev. B **69**, 113311 (2004).

[45] G. M. Minkov, O. E. Rut, A. A. Sherstobitov, S. A. Dvoretski, N. N. Mikhailov, V. A. Solov'ev, M. Y. Chernov, S. V. Ivanov, and A. V. Germanenko, Magneto-intersubband oscillations in two-dimensional systems with an energy spectrum split due to spin-orbit interaction, Phys. Rev. B **101**, 245303 (2020).

[46] A. Isihara and L. Smrčka, Density and magnetic field dependences of the conductivity of two-dimensional electron systems, J. Phys. C: Solid State Phys. **19**, 6777 (1986).

[47] P. D. Grigoriev and T. I. Mogilyuk, Magnetic quantum oscillations of in-plane Hall conductivity and magnetoresistance tensor in quasi-two-dimensional metals, arXiv:2312.07496.

[48] T. I. Mogilyuk and P. D. Grigoriev, Magnetic oscillations of in-plane conductivity in quasi-two-dimensional metals, Phys. Rev. B **98**, 045118 (2018).

[49] P. D. Grigoriev *et al.* (to be published).

[50] M. Fowler and R. E. Prange, Electron-phonon renormalization effects in high magnetic fields, Phys. Phys. Fiz. **1**, 315 (1965).

[51] S. Engelsberg and G. Simpson, Influence of electron-phonon interactions on the de Haas-van Alphen effect, Phys. Rev. B **2**, 1657 (1970).

[52] G. W. Martin, D. L. Maslov, and M. Yu. Reizer, Quantum magneto-oscillations in a two-dimensional Fermi liquid, Phys. Rev. B **68**, 241309(R) (2003).

[53] Y. Adamov, I. V. Gornyi, and A. D. Mirlin, Interaction effects on magneto-oscillations in a two-dimensional electron gas, Phys. Rev. B **73**, 045426 (2006).

[54] A. V. Chubukov and D. L. Maslov, First-Matsubara-frequency rule in a Fermi liquid. I. Fermionic self-energy, Phys. Rev. B **86**, 155136 (2012).

[55] M. V. Kartsovnik, P. D. Grigoriev, W. Biberacher, N. D. Kushch, and P. Wyder, Slow oscillations of magnetoresistance in quasi-two-dimensional metals, Phys. Rev. Lett. **89**, 126802 (2002).

[56] P. D. Grigoriev, Theory of the Shubnikov–de Haas effect in quasi-two-dimensional metals, Phys. Rev. B **67**, 144401 (2003).

[57] P. D. Grigoriev and T. Ziman, Slow quantum oscillations without fine-grained Fermi surface reconstruction in cuprate superconductors, JETP Lett. **106**, 371 (2017).

[58] P. D. Grigoriev and T. Ziman, Magnetic oscillations measure interlayer coupling in cuprate superconductors, Phys. Rev. B **96**, 165110 (2017).

[59] P. D. Grigoriev, M. V. Kartsovnik, and W. Biberacher, Magnetic-field-induced dimensional crossover in the organic metal α-(BEDT-TTF)$_2$KHg(SCN)$_4$, Phys. Rev. B **86**, 165125 (2012).

[60] M. E. Raikh and T. V. Shahbazyan, Magnetointersubband oscillations of conductivity in a two-dimensional electronic system, Phys. Rev. B **49**, 5531 (1994).

[61] N. S. Averkiev, L. E. Golub, S. A. Tarasenko, and M. Willander, Theory of magneto-oscillation effects in quasi-two-dimensional semiconductor structures, J. Phys.: Condens. Matter **13**, 2517 (2001).

[62] A. V. Goran, A. A. Bykov, A. I. Toropov, and S. A. Vitkalov, Effect of electron-electron scattering on magnetointersubband resistance oscillations of two-dimensional electrons in GaAs quantum wells, Phys. Rev. B **80**, 193305 (2009).

[63] S. Abedi, S. Vitkalov, A. A. Bykov, and A. K. Bakarov, Temperature damping of magneto-intersubband resistance oscillations in magnetically entangled subbands, Phys. Rev. B **104**, 075416 (2021).

[64] V. Leeb and J. Knolle, Theory of difference-frequency quantum oscillations, Phys. Rev. B **108**, 054202 (2023).